

Magnetized hot neutron matter: lowest order constrained variational calculations

G.H. Bordbar^{1,2 *}, Z. Rezaei¹

¹*Department of Physics,
Shiraz University, Shiraz 71454, Iran[†],*

and

²*Research Institute for Astronomy and Astrophysics of Maragha,
P.O. Box 55134-441,
Maragha 55177-36698, Iran*

Abstract

We have studied the spin polarized hot neutron matter in the presence of strong magnetic field. In this work, using the lowest order constrained variational method at finite temperature and employing AV_{18} nuclear potential, some thermodynamic properties of spin polarized neutron matter such as spin polarization parameter, free energy, equation of state and effective mass have been calculated. It has been shown that the strong magnetic field breaks the symmetry of the free energy, leading to a magnetized equilibrium state. We have found that the equation of state becomes stiffer by increasing both magnetic field and temperature. The magnetic field dependence of effective mass for the spin-up and spin-down neutrons has been investigated.

* Corresponding author. E-mail: bordbar@physics.susc.ac.ir

[†] Permanent address

I. INTRODUCTION

Based on the supernova models, after the gravitational collapse of a degenerate stellar core and the explosive ejection of outer layers material, a protoneutron star would be born [1]. Through the formation of the protoneutron star, the system arrives at a temperature of about $20 - 50 \text{ MeV}$ [2]. This protoneutron star is hot, opaque to neutrinos, and larger than an ordinary neutron star [1]. After the formation of the protoneutron star, neutrino emission is the dominant process in cooling of the neutron star (mainly by URCA process and neutrino Bremsstrahlung) [2].

Woltjer has predicted a magnetic field strength of order 10^{15} G for neutron stars as a result of the magnetic flux conservation from the progenitor star [3]. This in agreement with the experimental indication that the surface magnetic field strength of magnetars can be of the order $B_{magnetar} \approx 10^{14} - 10^{15} \text{ G}$ [4, 5]. The magnetic field can be distorted or amplified by some mixture of convection, differential rotation, and magnetic instabilities [6, 7]. The relative importance of these ingredients depends on the initial field strength and the rotation rate of the star. For both convection and differential rotation, the field and its supporting currents are not likely to be confined to the solid crust of the star but instead distributed in most of the stellar interior, which is mostly a fluid mixture of neutrons, protons, electrons, and other more exotic particles [8]. Thompson et al. argued that newborn neutron stars probably combine vigorous convection and differential rotation, making it likely that a dynamo process might operate in them [9]. They expected fields up to $10^{15} - 10^{16} \text{ G}$ in neutron stars with few-millisecond initial periods. In the core of high density inhomogeneous gravitationally bound neutron stars, the magnetic field strength can be as large as 10^{20} G [10]. In addition, considering the formation of a quark core in the high density interior of a neutron star, the maximum field reaches up to about 10^{20} G [10, 11]. According to the scalar virial theorem based on Newtonian gravity, the magnetic field strength is allowed to be up to 10^{18} G in the interior of a magnetar [12]. Moreover, general relativity predicts the allowed maximum value of the neutron star magnetic field to be $10^{18} - 10^{20} \text{ G}$ [13]. By comparing the cooling curves of neutron stars with the observational data, Yuan et al. obtained the magnetic field strength of order 10^{19} G for many not so old neutron stars [14].

The finite temperature and strong magnetic field in the interior of a protoneutron star can influence different astrophysical quantities. Therefore, to have a better understanding of

different astrophysical phenomena such as supernova explosion, thermal evolution and cooling of protoneutron stars, gravitational wave emission spectrum from neutron star mergers, and to get the more precise astrophysical quantities such as properties of very young hot neutron stars and composition of neutron stars, one should consider the neutron star matter at finite temperatures (excited neutron star matter) and strong magnetic fields.

Since β -equilibrium leads to an increase in the number of neutrons in neutron star matter, it is possible to approximate the neutron star matter by the pure neutron matter. Many works have dealt with the study of dense neutron matter at finite temperature [15–20]. Alonso et al. have used a field theoretical model for the analysis of relativistic neutron matter [15]. By solving the model in the renormalized Hartree approximation, they have investigated the effect of central temperature on the maxima of mass for stable configurations, the radii of the configurations, and the gravitational red shift at the surface of a neutron star. Panda et al. used a mean-field description of nonoverlapping nucleon bags bound by the self-consistent exchange of σ , ω , and ρ mesons to investigate the properties of neutron matter at finite temperature [16]. They showed that by increasing the temperature, the equation of state becomes stiffer. Within the framework of the Brueckner-Hartree-Fock formalism and using the AV_{18} nucleon-nucleon interaction for the spin polarized neutron matter, Bombaci et al. found that an increase in the temperature moderately affects the single-particle potentials [17]. In the Hartree-Fock approximation using Skyrme type interactions for spin polarized neutron matter, Rios et al. showed that the critical density at which the ferromagnetism takes place, decreases by temperature [18]. Within the self-consistent Green's-function approach applying the CD Bonn and the AV_{18} potential for neutron matter, Rios et al. found that the effect of dynamical correlations on the macroscopic properties is rather insensitive to the thermal effects [19]. The variational theory for fermions at finite temperature and high density has been applied by Mukherjee to neutron matter [20]. It has been found that the temperature dependence of the correlation operator is weak, but it is not negligible. Besides, it has been shown that the first order phase transition due to neutral pion condensation has a critical temperature of about $22MeV$ for neutron matter. The effect of strong magnetic field on the properties of dense neutron matter has also been considered. Perez-Garcia showed that for the neutron matter in the presence of strong magnetic fields, in the Skyrme model, there is a ferromagnetic phase transition at $\rho \sim 4\rho_0$, whereas it is forbidden in the $D1P$ model [21]. The results indicate that the effects of temperature on

the neutron magnetization remain moderate at temperatures up to about $T = 40 \text{ MeV}$. In the context of the Landau theory of normal Fermi liquids, using Skyrme and Gogny effective interactions, some thermodynamical quantities such as isothermal compressibility and spin susceptibility of pure neutron matter have also been studied [22].

In our previous works, we have investigated the spin polarized neutron matter [23], symmetric nuclear matter [24], asymmetric nuclear matter as well as neutron star matter [25] and magnetized neutron matter [26] at zero temperature using lowest order constrained variational (LOCV) method with the realistic strong interactions. We have also investigated the thermodynamic properties of spin polarized neutron matter [27], symmetric nuclear matter [28], and asymmetric nuclear matter [29] at finite temperature with no magnetic field. In the present work, we calculate different thermodynamic properties of spin polarized neutron matter at finite temperature in the presence of strong magnetic field using LOCV technique employing AV_{18} potential.

II. LOCV FORMALISM FOR THE SPIN POLARIZED HOT NEUTRON MATTER IN THE PRESENCE OF MAGNETIC FIELD

We consider a homogeneous system of N interacting particles with $N^{(+)}$ spin-up and $N^{(-)}$ spin-down neutrons under the influence of a uniform magnetic field, i.e. $\mathbf{B} = B\hat{k}$. The number densities of spin-up and spin-down neutrons are presented by $\rho^{(+)}$ and $\rho^{(-)}$ respectively. We introduce the spin polarization parameter, δ , by

$$\delta = \frac{\rho^{(+)} - \rho^{(-)}}{\rho}, \quad (1)$$

where $-1 \leq \delta \leq 1$, and ρ is the total number density of system. The magnetization density of neutron matter is defined as

$$m = \mu_n \delta \rho, \quad (2)$$

where μ_n is the neutron magnetic moment. The total magnetization of a given volume is also as follows

$$M = \int m dV. \quad (3)$$

In order to calculate the energy of this system, we use LOCV method as follows: we consider a trial many-body wave function of the form

$$\psi = \mathcal{F}\phi, \quad (4)$$

where ϕ is the uncorrelated ground-state wave function of N independent neutrons, and \mathcal{F} is a proper N -body correlation function. Using Jastrow approximation [30], \mathcal{F} can be replaced by

$$\mathcal{F} = S \prod_{i>j} f(ij), \quad (5)$$

where S is a symmetrizing operator. We consider a cluster expansion of the energy functional up to the two-body term,

$$E([f]) = \frac{1}{N} \frac{\langle \psi | H | \psi \rangle}{\langle \psi | \psi \rangle} = E_1 + E_2. \quad (6)$$

The one-body term, E_1 , is given by

$$E_1 = -\frac{MH}{N} + \sum_{i=+,-} \bar{\varepsilon}_i, \quad (7)$$

where the first term of Eq. (7), H shows the external magnetic field. It should be noted that we have used B to present the magnetic field strength; while the total magnetic field is the sum of the external magnetic field and the induced magnetization, $B = H + 4\pi M$. Because of the tiny value of the neutron magnetic moment, we assume that the induced magnetization has a small contribution to the total magnetic field. Consequently,

$$B \sim H. \quad (8)$$

Using Eqs. (2), (3) and (8), the one-body term can be written as

$$E_1 = -\mu_n B \delta + \sum_{i=+,-} \bar{\varepsilon}_i. \quad (9)$$

The second term in Eq. (7), $\bar{\varepsilon}_i$ is as follows

$$\bar{\varepsilon}_i = \sum_k \frac{\hbar^2 k^2}{2m} \bar{n}_i(k, T, B, \rho^{(i)}), \quad (10)$$

where $\bar{n}_i(k, T, B, \rho^{(i)})$ is the Fermi-Dirac distribution function in the presence of magnetic field,

$$\bar{n}_i(k, T, B, \rho^{(i)}) = \frac{1}{e^{\beta[\bar{\varepsilon}_i(k, T, B, \rho^{(i)}) - \bar{\mu}_i(T, B, \rho^{(i)})]} + 1}. \quad (11)$$

In Eq. (11), $\bar{\epsilon}_i$ and $\bar{\mu}_i$ are the single-particle energy of a neutron and the neutron chemical potential respectively. The single-particle energy, $\bar{\epsilon}_i$, of a neutron with momentum k and spin projection i in the presence of magnetic field is approximately written in terms of the effective mass as follows [18]

$$\bar{\epsilon}_i(k, T, B, \rho^{(i)}) = \begin{cases} \frac{\hbar^2 k^2}{2m_+^*(T, \rho)} - \mu_n B + U_+(T, \rho^{(+)}) ; & i = +, \\ \frac{\hbar^2 k^2}{2m_-^*(T, \rho)} + \mu_n B + U_-(T, \rho^{(-)}) ; & i = -. \end{cases} \quad (12)$$

In fact, we use a quadratic approximation for the single particle potential incorporated in the single particle energy as a momentum independent effective mass. $U_i(T, \rho^{(i)})$ is the momentum independent single particle potential. The effective mass, m_i^* , is determined variationally [31–35]. The chemical potential, $\bar{\mu}_i$, is also obtained by applying the constraint

$$\sum_k \bar{n}_i(k, T, B, \rho^{(i)}) = N^{(i)}. \quad (13)$$

The two-body energy, E_2 , is

$$E_2 = \frac{1}{2N} \sum_{ij} \langle ij | \nu(12) | ij - ji \rangle, \quad (14)$$

where

$$\nu(12) = -\frac{\hbar^2}{2m} [f(12), [\nabla_{12}^2, f(12)]] + f(12)V(12)f(12).$$

$f(12)$ and $V(12)$ are the two-body correlation function and nuclear potential respectively. In the LOCV formalism, the two-body correlation function, $f(12)$, is considered as follows [36],

$$f(12) = \sum_{k=1}^3 f^{(k)}(r_{12})P_{12}^{(k)}, \quad (15)$$

where

$$P_{12}^{(k=1-3)} = \left(\frac{1}{4} - \frac{1}{4}\sigma_1 \cdot \sigma_2\right), \left(\frac{1}{2} + \frac{1}{6}\sigma_1 \cdot \sigma_2 + \frac{1}{6}S_{12}\right), \left(\frac{1}{4} + \frac{1}{12}\sigma_1 \cdot \sigma_2 - \frac{1}{6}S_{12}\right). \quad (16)$$

In Eq. (16), S_{12} and $\sigma_1 \cdot \sigma_2$ are the tensor and Pauli operators respectively. Using the above two-body correlation function and the AV_{18} two-body potential [37], after doing some

algebra, we find the following equation for the two-body energy:

$$\begin{aligned}
E_2 = & \frac{2}{\pi^4 \rho} \left(\frac{\hbar^2}{2m} \right) \sum_{JLSSz} \frac{(2J+1)}{2(2S+1)} [1 - (-1)^{L+S+1}] \left| \left\langle \frac{1}{2} \sigma_{z1} \frac{1}{2} \sigma_{z2} \mid SSz \right\rangle \right|^2 \times \\
& \times \int dr \left\{ \left[f_\alpha^{(1)'}{}^2 a_\alpha^{(1)2}(r, \rho, T) \right. \right. \\
& + \frac{2m}{\hbar^2} (\{V_c - 3V_\sigma + V_\tau - 3V_{\sigma\tau} + 2(V_T - 3V_{\sigma T}) - 2V_{\tau z}\} a_\alpha^{(1)2}(r, \rho, T) \\
& + [V_{l2} - 3V_{l2\sigma} + V_{l2\tau} - 3V_{l2\sigma\tau}] c_\alpha^{(1)2}(r, \rho, T) (f_\alpha^{(1)})^2] + \sum_{k=2,3} \left[f_\alpha^{(k)'}{}^2 a_\alpha^{(k)2}(r, \rho, T) \right. \\
& + \frac{2m}{\hbar^2} (\{V_c + V_\sigma + V_\tau + V_{\sigma\tau} + (-6k+14)(V_{t\tau} + V_t) - (k-1)(V_{ls\tau} + V_{ls}) \\
& + 2[V_T + V_{\sigma T} + (-6k+14)V_{tT} - V_{\tau z}]\} a_\alpha^{(k)2}(r, \rho, T) \\
& + [V_{l2} + V_{l2\sigma} + V_{l2\tau} + V_{l2\sigma\tau}] c_\alpha^{(k)2}(r, \rho, T) + [V_{ls2} + V_{ls2\tau}] d_\alpha^{(k)2}(r, \rho, T) (f_\alpha^{(k)})^2] \\
& + \frac{2m}{\hbar^2} \{V_{ls} + V_{ls\tau} - 2(V_{l2} + V_{l2\sigma} + V_{l2\sigma\tau} + V_{l2\tau}) - 3(V_{ls2} + V_{ls2\tau})\} b_\alpha^2(r, \rho, T) f_\alpha^{(2)} f_\alpha^{(3)} \\
& \left. \left. + \frac{1}{r^2} (f_\alpha^{(2)} - f_\alpha^{(3)})^2 b_\alpha^2(r, \rho, T) \right\}, \tag{17}
\end{aligned}$$

where $\alpha = \{J, L, S, S_z\}$ and the coefficients $a_\alpha^{(i)2}$, b_α^2 , $c_\alpha^{(i)2}$, and $d_\alpha^{(i)2}$ are defined as

$$a_\alpha^{(1)2}(r, \rho, T) = r^2 I_{L, S_z}(r, \rho, T), \tag{18}$$

$$a_\alpha^{(2)2}(r, \rho, T) = r^2 [\beta I_{J-1, S_z}(r, \rho, T) + \gamma I_{J+1, S_z}(r, \rho, T)], \tag{19}$$

$$a_\alpha^{(3)2}(r, \rho, T) = r^2 [\gamma I_{J-1, S_z}(r, \rho, T) + \beta I_{J+1, S_z}(r, \rho, T)], \tag{20}$$

$$b_\alpha^2(r, \rho, T) = r^2 [\beta_{23} I_{J-1, S_z}(r, \rho, T) - \beta_{23} I_{J+1, S_z}(r, \rho, T)], \tag{21}$$

$$c_\alpha^{(1)2}(r, \rho, T) = r^2 \nu_1 I_{L, S_z}(r, \rho, T), \tag{22}$$

$$c_\alpha^{(2)2}(r, \rho, T) = r^2 [\eta_2 I_{J-1, S_z}(r, \rho, T) + \nu_2 I_{J+1, S_z}(r, \rho, T)], \tag{23}$$

$$c_\alpha^{(3)2}(r, \rho, T) = r^2 [\eta_3 I_{J-1, S_z}(r, \rho, T) + \nu_3 I_{J+1, S_z}(r, \rho, T)], \tag{24}$$

$$d_\alpha^{(2)2}(r, \rho, T) = r^2 [\xi_2 I_{J-1, S_z}(r, \rho, T) + \lambda_2 I_{J+1, S_z}(r, \rho, T)], \tag{25}$$

$$d_\alpha^{(3)2}(r, \rho, T) = r^2[\xi_3 I_{J-1, S_z}(r, \rho, T) + \lambda_3 I_{J+1, S_z}(r, \rho, T)], \quad (26)$$

with

$$\beta = \frac{J+1}{2J+1}, \quad \gamma = \frac{J}{2J+1}, \quad \beta_{23} = \frac{2J(J+1)}{2J+1}, \quad (27)$$

$$\nu_1 = L(L+1), \quad \nu_2 = \frac{J^2(J+1)}{2J+1}, \quad \nu_3 = \frac{J^3 + 2J^2 + 3J + 2}{2J+1}, \quad (28)$$

$$\eta_2 = \frac{J(J^2 + 2J + 1)}{2J+1}, \quad \eta_3 = \frac{J(J^2 + J + 2)}{2J+1}, \quad (29)$$

$$\xi_2 = \frac{J^3 + 2J^2 + 2J + 1}{2J+1}, \quad \xi_3 = \frac{J(J^2 + J + 4)}{2J+1}, \quad (30)$$

$$\lambda_2 = \frac{J(J^2 + J + 1)}{2J+1}, \quad \lambda_3 = \frac{J^3 + 2J^2 + 5J + 4}{2J+1}, \quad (31)$$

and

$$I_{J, S_z}(r, \rho, T) = \frac{1}{2\pi^6 \rho^2} \int dk_1 dk_2 \bar{n}_i(k_m, T, B, \rho^{(i)}) \bar{n}_j(k_m, T, B, \rho^{(j)}) J_J^2(|k_2 - k_1|r). \quad (32)$$

In the above equation, $J_J(x)$ is the Bessel function.

Now, we minimize the two-body energy with respect to the variations in the function $f_\alpha^{(i)}$ subject to the normalization constraint,

$$\frac{1}{N} \sum_{ij} \langle ij | h_{S_z}^2 - f^2(12) | ij \rangle_a = 0. \quad (33)$$

The minimization subject to the above normalization constraint leads to the normalization of the two body wave function to unity [36]. For the spin polarized hot neutron matter, the function $h_{S_z}(r)$ is defined as follows,

$$h_{S_z}(r) = \begin{cases} \left[1 - \left(\frac{\gamma_i(r)}{\rho} \right)^2 \right]^{-1/2} & ; \quad S_z = \pm 1, \\ 1 & ; \quad S_z = 0, \end{cases} \quad (34)$$

where

$$\gamma_i(r) = \frac{1}{2\pi^2} \int dk \bar{n}_i(k_m, T, B, \rho^{(i)}) J_0(kr) k^2. \quad (35)$$

From the minimization of the two-body cluster energy, we get a set of coupled and uncoupled differential equations [38]. By solving these equations, we can obtain the correlation functions to compute the two-body energy term, E_2 . As the final step, we calculate the free energy per particle, F , to get different thermodynamic properties of spin polarized hot neutron matter,

$$F(\rho, T, B) = E(\rho, T, B) - TS(\rho, T, B), \quad (36)$$

where S is the entropy per particle,

$$S(\rho, T, B) = -\frac{1}{N} \sum_{i=+,-} \sum_k \{ [1 - \bar{n}_i(k, T, B, \rho^{(i)})] \ln [1 - \bar{n}_i(k, T, B, \rho^{(i)})] + \bar{n}_i(k, T, B, \rho^{(i)}) \ln [\bar{n}_i(k, T, B, \rho^{(i)})] \}. \quad (37)$$

It should be noted that in our calculations, we introduce the effective masses, m_i^* , as variational parameters [31–35]. We minimize the free energy with respect to the variations in the effective masses, and then we obtain the chemical potentials and the effective masses of spin-up and spin-down neutrons at the equilibrium state. In our approach, the effective mass depends on both density and temperature but it is independent of the momentum. The effective mass of a quasiparticle near the Fermi surface for the spin polarized neutron matter at low temperatures is also the static physical quantity of interest in the context of Landau Fermi liquid theory [39].

III. RESULTS AND DISCUSSION

In Fig. 1, we present the free energy per particle of spin polarized neutron matter versus the spin polarization parameter δ . Fig. 1a shows that in the presence of magnetic field, the free energy is not a symmetric function of spin polarization parameter and the equilibrium configuration would experience a net magnetization. Clearly, the effects of magnetic fields below $B \sim 10^{18} G$ are almost insignificant, but by increasing the magnetic field, the equilibrium value of the spin polarization parameter (i.e. the polarization that minimizes the free energy) and the free energy decrease, leading to a more stable system. Fig. 1b indicates that the effect of temperature on the fully spin polarized neutron matter is less than that of the unpolarized one.

Fig. 2 presents the equilibrium value of the spin polarization parameter versus density ρ . Fig. 2a shows that at low densities ($\rho \leq 0.2 \text{ fm}^{-3}$), the magnitude of the spin polarization parameter decreases by increasing the temperature. However, at higher densities, the related values of the spin polarization parameter at different finite temperatures are almost identical to the one for zero temperature. This is due to smaller values of T/ε_f^* at high densities (Fig. 2b), in which ε_f^* is defined as follows,

$$\varepsilon_f^* = \sum_{i=+,-} \frac{\rho^{(i)}}{\rho} \varepsilon_{fi}^*, \quad (38)$$

with

$$\varepsilon_{f+}^* = \frac{\hbar^2 k_F^{(+)^2}}{2m} - \mu_n B, \quad (39)$$

and

$$\varepsilon_{f-}^* = \frac{\hbar^2 k_F^{(-)^2}}{2m} + \mu_n B. \quad (40)$$

In the above equations, ε_{fi}^* and $k_F^{(i)} = (6\pi^2 \rho^{(i)})^{1/3}$ are the Fermi energy and Fermi momentum of neutrons with spin projection i in the presence of the magnetic field. It is evident from Eq. (38) that ε_f^* gives an average of the Fermi energy of magnetized neutron matter. Therefore, the ratio T/ε_f^* is a criterion for the fraction of particles which are thermally excited [40], and how much the system is disordered. In Fig. 3, we show the spin polarization parameter at the equilibrium state as a function of the magnetic field B . At each temperature, the magnitude of spin polarization parameter grows by increasing the magnetic field (Fig. 3a). We have found that at strong magnetic fields, the effect of finite temperature is more significant because the ratio T/ε_f^* rises with the increase in the magnetic field (Fig. 3b).

The free energy per particle at the equilibrium value of the spin polarization parameter is presented in Fig. 4. It can be seen that at finite temperature, the free energy is an increasing function of density (Fig. 4a). At low densities, the rate of increase in the free energy varies by increasing the density, but at high densities, this rate of increase is nearly constant. Moreover, the effect of temperature on the free energy is more pronounced at low densities. Fig. 4b shows that the free energy decreases by growing the temperature nearly at the same rate for different magnetic fields. The free energy decreases by increasing the magnetic field (Fig. 4c). We can see that by increasing the magnetic field up to a value of about $B \simeq 10^{18} \text{ G}$, the free energy per particle slowly decreases, and then it rapidly decreases

for the magnetic fields greater than this value. This indicates that, above $B \simeq 10^{18} G$, the effect of magnetic field on the free energy of the spin polarized neutron matter becomes more important.

From the free energy per particle of magnetized neutron matter, F , we can obtain the corresponding pressure of neutron matter using the following relation,

$$P(\rho, T, B) = \rho^2 \left(\frac{\partial F(\rho, T, B)}{\partial \rho} \right)_{T, B}. \quad (41)$$

This equation of state (EoS) is plotted in Fig. 5. For each value of the density, pressure increases by growing the magnetic field (Fig. 5a). This stiffening of the equation of state is due to the inclusion of neutron anomalous magnetic moments. From the astrophysical point of view, it should be noted that this stiffening of the EoS leads to the larger value for the maximum mass of neutron star [41–43]. At each density, the pressure at finite temperature is larger than that of zero temperature (Fig. 5b). It means that the equation of state of neutron matter becomes stiffer by increasing the temperature. Fig. 5c also shows that by increasing the temperature, the pressure increases nearly at the same rate for different magnetic fields.

Fig. 6 shows the effective mass corresponding with the equilibrium of the system for the spin-up and spin-down neutrons as a function of the magnetic field B . At low magnetic fields, the effective masses of spin-up and spin-down neutrons are nearly identical because the effective masses of spin-up and spin-down neutrons have the same values at $\delta \simeq 0$. Fig. 6 indicates that the effective mass of spin-up (spin-down) neutrons decreases (increases) by increasing the magnetic field in agreement with the results obtained in Ref. [22]. From the comparison of Fig. 3a and 6, we can see that the shift in mass is due to the polarization of neutron matter. For the maximum value of the magnetic field considered in this work, i.e. $5 \times 10^{18} G$, and at $T = 10 MeV$ and $\rho = 0.3 fm^{-3}$, the equilibrium value of the spin polarization parameter is about $\delta_{B_{max}} = -0.23$ and that corresponds to a mass shift of an amount of $\Delta(m^*/m) \approx 0.02$ with respect to the unpolarized case.

IV. SUMMARY AND CONCLUDING REMARKS

We have investigated the effect of strong magnetic fields on the thermodynamic properties of spin polarized hot neutron matter applying LOCV method and using AV_{18} potential. We

have found that in the presence of a strong magnetic field, the free energy is not a symmetric function of the spin polarization parameter and the system is macroscopically magnetized. By increasing both density and temperature, the magnitude of the equilibrium value of the spin polarization parameter decreases. At low magnetic fields, the free energy decreases very slowly by increasing the magnetic field, but at stronger magnetic fields, the free energy decreases rapidly with the increase in the magnetic field. It has been found that the equation of state becomes stiffer by increasing the magnetic field. This stiffening of the EoS leads to the larger value for the maximum mass of neutron star.

Acknowledgments

We wish to thank the Research Institute for Astronomy and Astrophysics of Maragha and Shiraz University Research Council.

-
- [1] P. Haensel, A.Y. Potekhin, and D.G. Yakovlev, *Neutron Stars 1: Equation of State and Structure*, Springer Science, 2007.
 - [2] M. Camenzind, *Compact Objects in Astrophysics: White Dwarfs, Neutron Stars and Black Holes*, Springer, Verlag Berlin Heidelberg, 2007.
 - [3] L. Woltjer, *Astrophys. J.* 140 (1964) 1309.
 - [4] C. Thompson and R. C. Duncan, *Mon. Not. R. Astron. Soc.* 275 (1995) 255.
 - [5] D. Lazzati, *Nature* 434 (2005) 1075.
 - [6] R.J. Tayler, *MNRAS* 161 (1973) 365.
 - [7] H. Spruit, *Astron. Astrophys.* 381 (2002) 923.
 - [8] A. Reisenegger, *Astron. Nachr.* 328 (2007) 1173.
 - [9] C. Thompson and R. C. Duncan, *Astrophys. J.* 408 (1993) 194.
 - [10] E.J. Ferrer, V. de la Incera, J.P. Keith, I. Portillo and P.L. Springsteen, *Phys. Rev. C* 82 (2010) 065802.
 - [11] T. Tatsumi, *Phys. Lett. B* 489 (2000) 280.
 - [12] D. Lai and S. L. Shapiro, *Astrophys. J.* 383 (1991) 745.
 - [13] S. Shapiro and S. Teukolsky, *Black Holes, White Dwarfs and Neutron Stars*, Wiley, New York,

1983.

- [14] Y. F. Yuan and J. L. Zhang , *Astron. Astrophys.* 335 (1998) 969.
- [15] J. D. Alonso, J. M. Ibanez and H. Sivak, *Phys. Rev. C* 39 (1989) 671.
- [16] P. K. Panda, R. Sahu and C. Das, *Phys. Rev. C* 60 (1999) 038801.
- [17] I. Bombaci, A. Polls, A. Ramos, A. Rios and I. Vidana, *Phys. Lett. B* 632 (2006) 638.
- [18] A. Rios, A. Polls and I. Vidana, *Phys. Rev. C* 71 (2005) 055802.
- [19] A. Rios, A. Polls and I. Vidana, *Phys. Rev. C* 79 (2009) 025802.
- [20] A. Mukherjee, *Phys. Rev. C* 79 (2009) 045811.
- [21] M. A. Perez-Garcia, *Phys. Rev. C* 77 (2008) 065806.
- [22] M. A. Perez-Garcia, J. Navarro and A. Polls, *Phys. Rev. C* 80 (2009) 025802.
- [23] G. H. Bordbar and M. Bigdeli, *Phys. Rev. C* 75 (2007) 045804.
- [24] G. H. Bordbar and M. Bigdeli, *Phys. Rev. C* 76 (2007) 035803.
- [25] G. H. Bordbar and M. Bigdeli, *Phys. Rev. C* 77 (2008) 015805.
- [26] G. H. Bordbar, Z. Rezaei and A. Montakhab, *Phys. Rev. C* 83 (2011) 044310.
- [27] G. H. Bordbar and M. Bigdeli, *Phys. Rev. C* 78 (2008) 054315.
- [28] M. Bigdeli, G. H. Bordbar and Z. Rezaei, *Phys. Rev. C* 80 (2009) 034310.
- [29] M. Bigdeli, G. H. Bordbar and A. Poostforush, *Phys. Rev. C* 82 (2010) 034309.
- [30] J. W. Clark, *Prog. Part. Nucl. Phys.* 2 (1979) 89.
- [31] M. Modarres, *J. Phys. G: Nucl. Part. Phys.* 19 (1993) 1349.
- [32] M. Modarres, *J. Phys. G: Nucl. Part. Phys.* 21 (1995) 351.
- [33] M. Modarres, *J. Phys. G: Nucl. Part. Phys.* 23 (1997) 923.
- [34] M. Modarres and G. H. Bordbar, *Phys. Rev. C* 58 (1998) 2781.
- [35] B. Friedman and V. R. Pandharipande, *Nucl. Phys. A* 361 (1981) 502.
- [36] J. C. Owen, R. F. Bishop, and J. M. Irvine, *Nucl. Phys. A* 277 (1977) 45.
- [37] R. B. Wiringa, V. G. J. Stoks, and R. Schiavilla, *Phys. Rev. C* 51 (1995) 38.
- [38] G. H. Bordbar and M. Modarres, *Phys. Rev. C* 57 (1998) 714.
- [39] L. Landau, *Sov. Phys. JETP* 3 (1957) 920.
- [40] R. K. Pathria, *Statistical Mechanics*, Pergamon Press, 1980.
- [41] G. H. Bordbar and M. Hayati, *Int. J. Mod. Phys. A* 21 (2006) 1555.
- [42] G. H. Bordbar, S. M. Zebarjad and R. Zahedinia, *Int. J. Theor. Phys.* 48 (2009) 61.
- [43] T. Yazdizadeh and G. H. Bordbar, *Res. Astron. Asrtophys.* 11 (2011) 471.

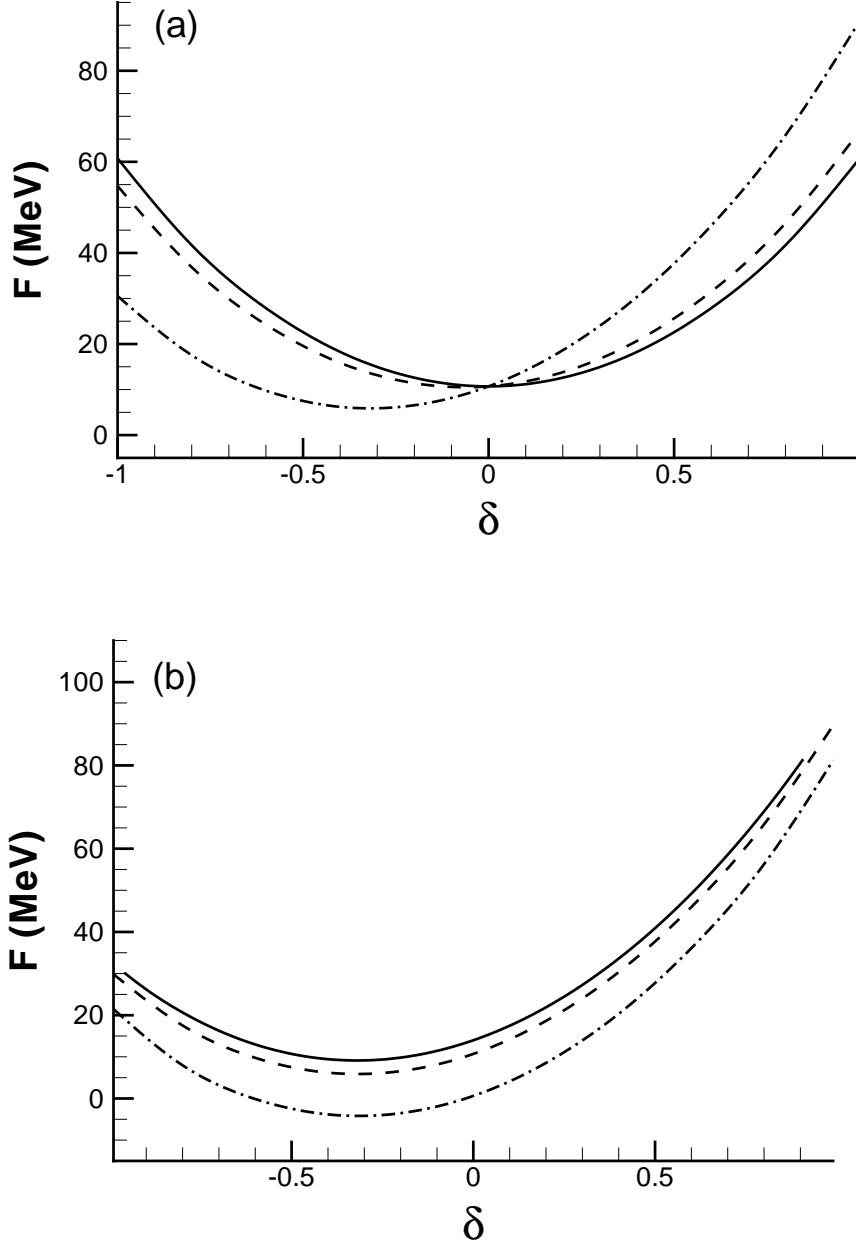


FIG. 1: Free energy per particle as a function of the spin polarization parameter δ : (a) for the cases $B = 0$ G (solid curve), $B = 10^{18}$ G (dashed curve) and $B = 5 \times 10^{18}$ G (dashdot curve) at the fixed values of the temperature, $T = 10$ MeV, and the density, $\rho = 0.2$ fm $^{-3}$, (b) for the cases $T = 0$ MeV (solid curve), $T = 10$ MeV (dashed curve) and $T = 20$ MeV (dashdot curve) at the fixed values of the magnetic field, $B = 5 \times 10^{18}$ G, and the density, $\rho = 0.2$ fm $^{-3}$.

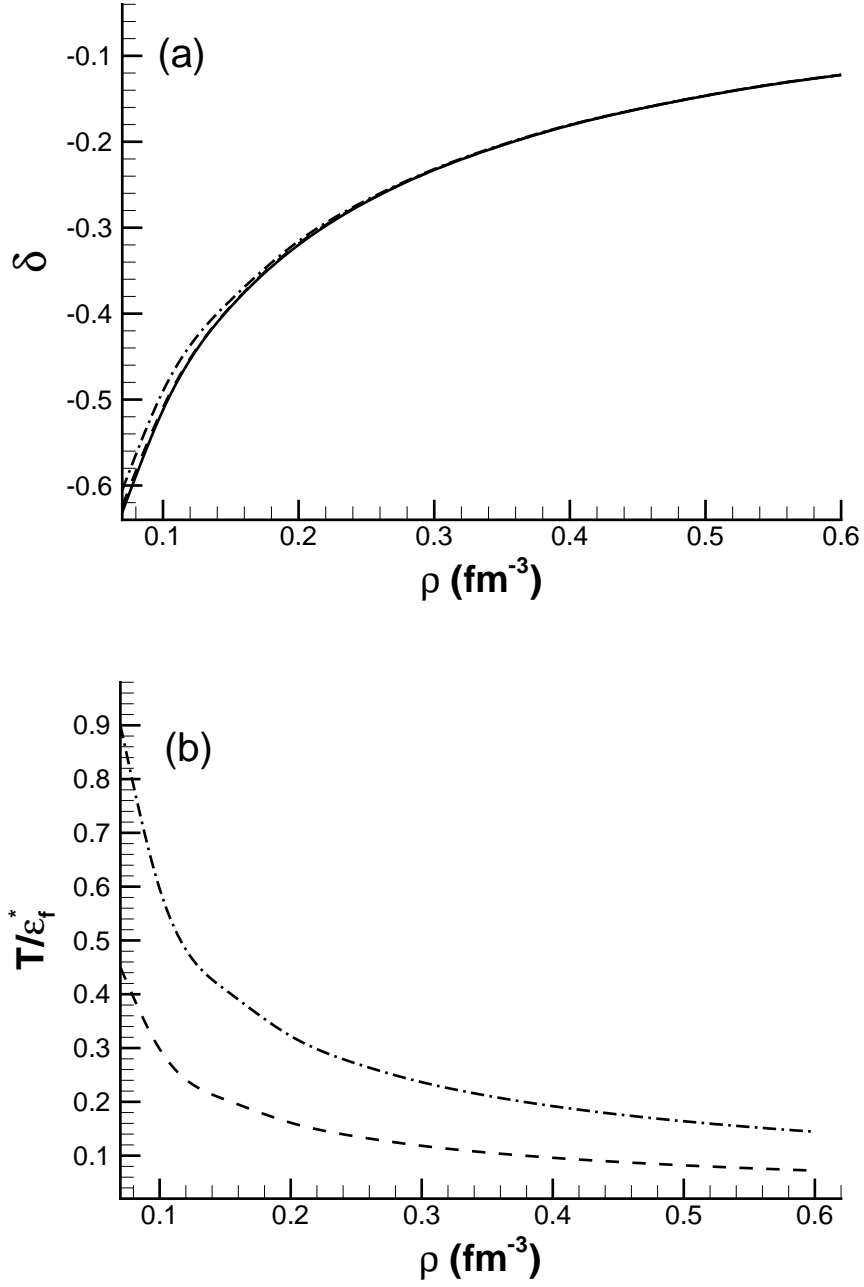


FIG. 2: (a) Spin polarization parameter at the equilibrium state as a function of the density ρ for the cases $T = 0 \text{ MeV}$ (solid curve), $T = 10 \text{ MeV}$ (dashed curve) and $T = 20 \text{ MeV}$ (dashdot curve), and a fixed value of the magnetic field, $B = 5 \times 10^{18} \text{ G}$. (b) Same as in the top panel but for the ratio T/ε_f^* .

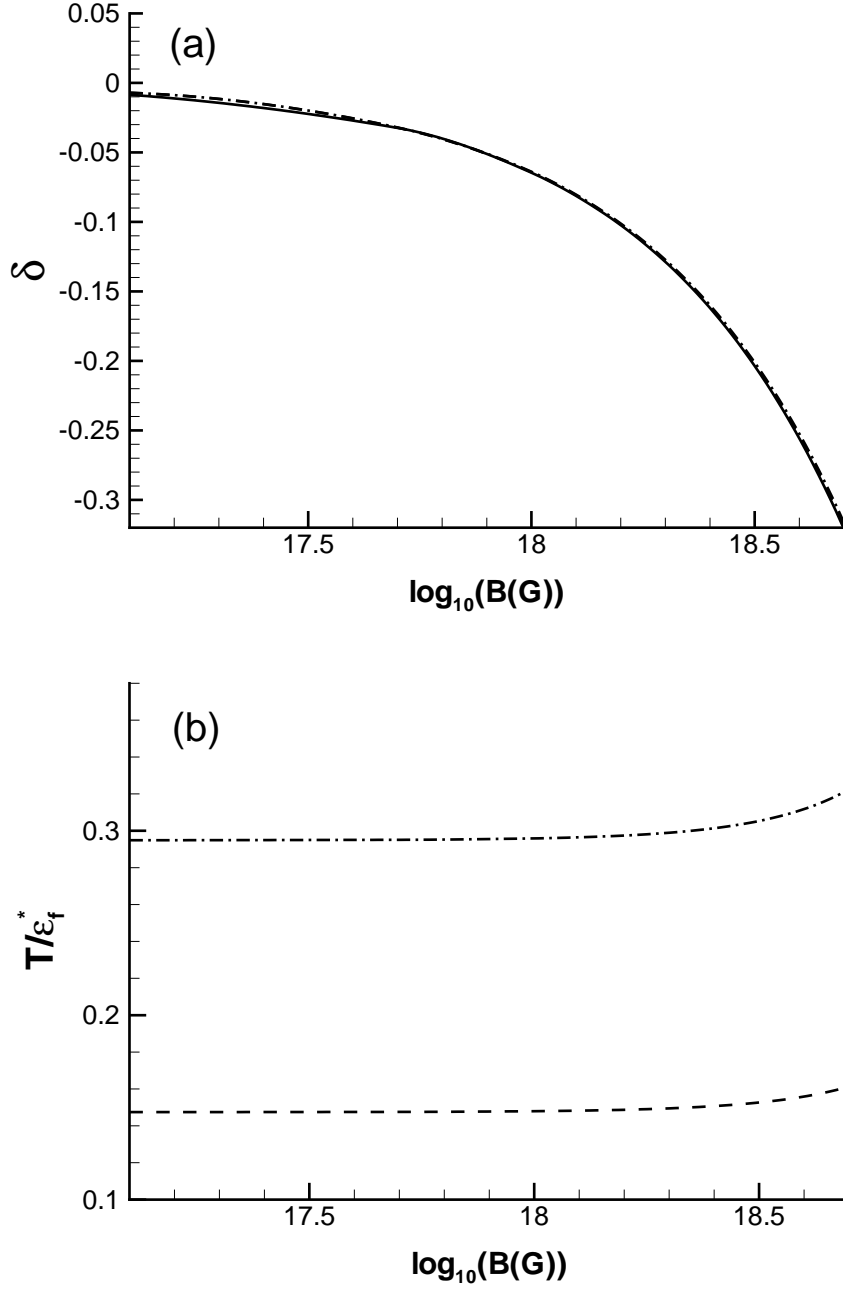


FIG. 3: (a) Magnetic field dependence of the spin polarization parameter δ at the equilibrium state for the cases $T = 0 \text{ MeV}$ (solid curve), $T = 10 \text{ MeV}$ (dashed curve) and $T = 20 \text{ MeV}$ (dashdot curve), and a fixed value of the density, $\rho = 0.2 \text{ fm}^{-3}$. (b) Same as in the top panel but for the ratio T/ϵ_f^* .

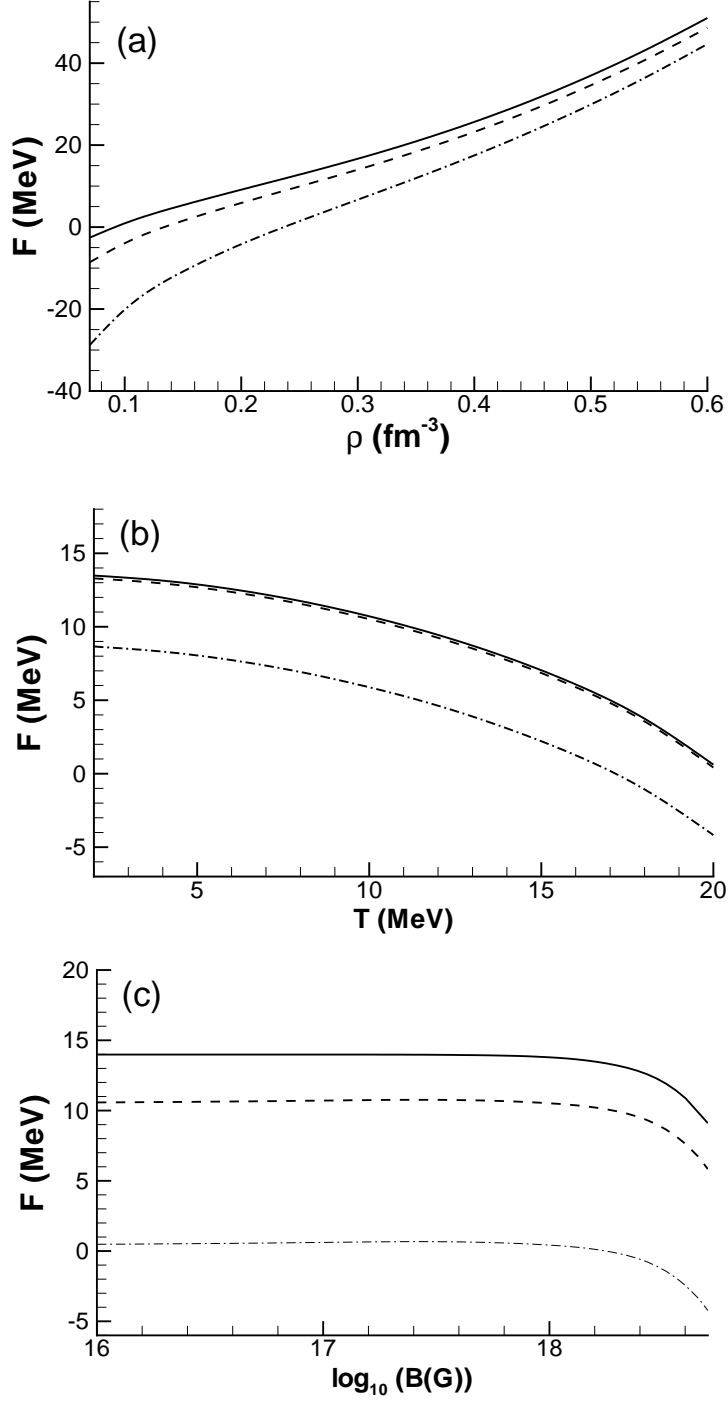


FIG. 4: Free energy per particle at the equilibrium state as a function of: (a) the density ρ for the cases $T = 0$ MeV (solid curve), $T = 10$ MeV (dashed curve) and $T = 20$ MeV (dashdot curve), and a fixed value of the magnetic field, $B = 5 \times 10^{18}$ G, (b) the temperature T for the cases $B = 0$ G (solid curve), $B = 10^{18}$ G (dashed curve) and $B = 5 \times 10^{18}$ G (dashdot curve), and a fixed value of the density, $\rho = 0.2 \text{ fm}^{-3}$, (c) the magnetic field B for the cases $T = 0$ MeV (solid curve), $T = 10$ MeV (dashed curve) and $T = 20$ MeV (dashdot curve), and a fixed value of the density, $\rho = 0.2 \text{ fm}^{-3}$.

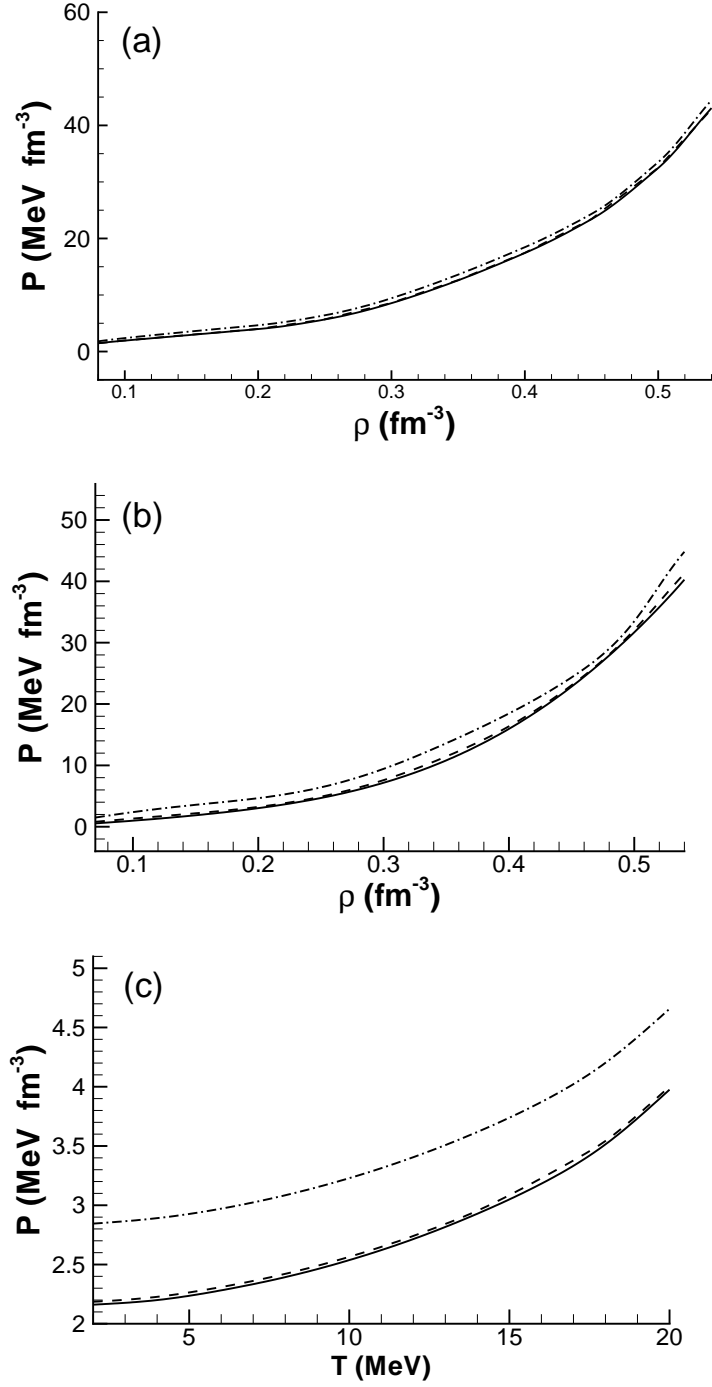


FIG. 5: Pressure of spin polarized neutron matter as a function of: (a) the density ρ for the cases $B = 0$ G (solid curve), $B = 10^{18}$ G (dashed curve) and $B = 5 \times 10^{18}$ G (dashdot curve), and a fixed value of the temperature, $T = 20$ MeV, (b) the density ρ for the cases $T = 0$ MeV (solid curve), $T = 10$ MeV (dashed curve) and $T = 20$ MeV (dashdot curve), and a fixed value of the magnetic field, $B = 5 \times 10^{18}$ G, (c) the temperature T for the cases $B = 0$ G (solid curve), $B = 10^{18}$ G (dashed curve) and $B = 5 \times 10^{18}$ G (dashdot curve), and a fixed value of the density, $\rho = 0.2$ fm^{-3} .

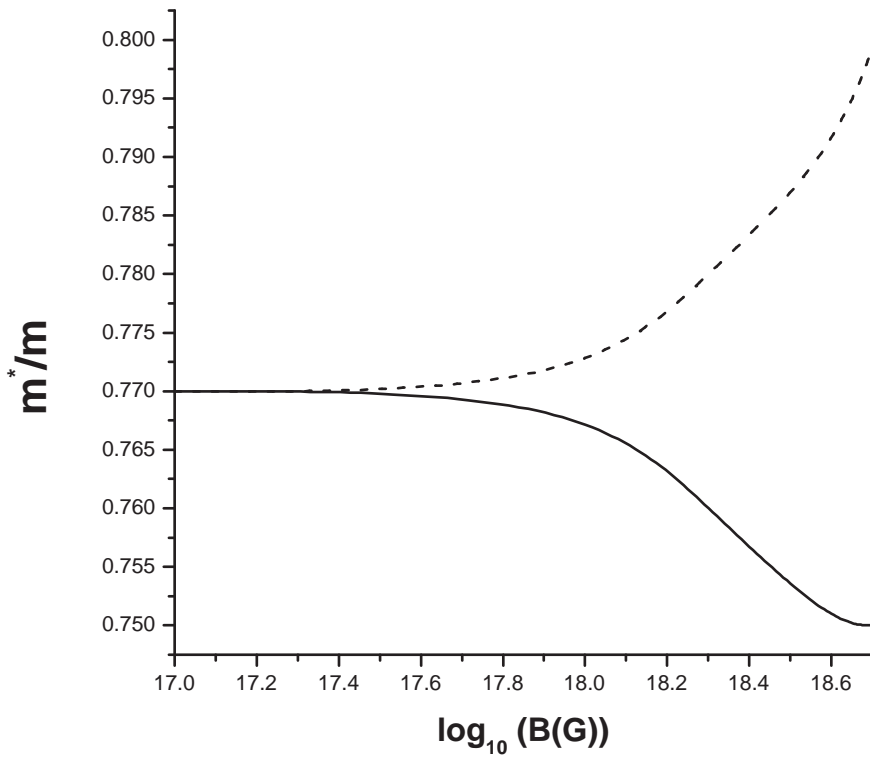


FIG. 6: Magnetic field dependence of the effective masses of spin-up (solid curve) and spin-down (dashed curve) neutrons corresponding with the equilibrium state at the fixed values of the temperature, $T = 10 \text{ MeV}$, and the density, $\rho = 0.3 \text{ fm}^{-3}$.